WESTERN PACIFIC EARTH SCIENCES
Vol.1, No.2, P.213-226, 12 Figs., May, 2001

STRUCTURAL EVOLUTION OF THE SOUTHEASTERN CENTRAL RANGE, TAIWAN

C. Y. LU[1],K. J. CHANG[2], J. MALAVIEILLE[2], Y.C. CHAN[3], C. P.CHANG[4] AND J. C. LEE[3]

1. Department of Geosciences, National Taiwan University, Taipei, Taiwan
2. Lab. Geophysics, Tectonics, and Sedimentology, Univ., Montpellier II, France
3. Institute of Earth Sciences, Academia Sinica, Taiwan
4. Departement de Geotectonique Univ. Pierre et Marie. Curie, Jussieu, France

ABSTRACT

The deformation structures of southeastern Taiwan reveal characteristics of early orogenic stages and transpressional tectonics, which are fundamentally significant mountain building processes of the island arc. Thick series of Miocene deposits in this area suffered lowest-grade metamorphism and ductile-brittle deformation during the Late Cenozoic orogeny. Field investigation and structural analysis allow characterization of the structures and reconstruction of the evolution of deformation in the Backbone Range fold-and-thrust belt. Three deformation stages can be distinguished: (1) the first stage involving an early west-vergent contraction and volume loss resulting in thrusting, regional tilting of strata, slumping and subsequent folding; (2) the second stage being dominated by general shear, which resulted in widespread east-vergent back-folding and back-thrusting associated with isoclinal folding; and (3) the third stage mainly involving transpression in association with E-W contractional thrusting and folding, as well as a new style of penetrative cleavage. Many of the well-characterized structures in the study area disappeared progressively towards the north. However, many early orogenic structures have been either obliterated or eroded away as the mountain belt became older due to oblique accretion.

Key words: structural evolution, SE Taiwan, transpressional tectonics, oblique accretion, early orogenic stages.

INTRODUCTION

The Taiwan Mountain Belt is one of the most active and youngest mountain belts on the Earth's surface. It results from the oblique convergence between the Eurasian plate and the

Philippine Sea plate (Biq, 1971; Biq, 1972; Chai, 1972; Suppe, 1981) (Fig.1). The convergence has propagated accretion of the Luzon arc southward and subsequently resulted in continental growth of the Asian continent. The convergence velocity has been estimated at 8.2cm/yr in the N54°W direction (Yu *et al.*, 1997). The Luzon arc trends N10°W whereas the Central Range trends N16°E. As its location is appropriated in the mountain belt, the southeastern Central Range of Taiwan can be considered as the best site for studying the early history of structural evolution.

The accretion of landmass at the southern end of the Coastal Range in combination with the oblique convergent tectonics and indentation of the forearc basement has provided a specific left-lateral right step transpressional environment in the southeastern Central Range. Therefore, the present paper attempts to describe the deformational structures and reveal the mountain building kinematics in this part of Taiwan.

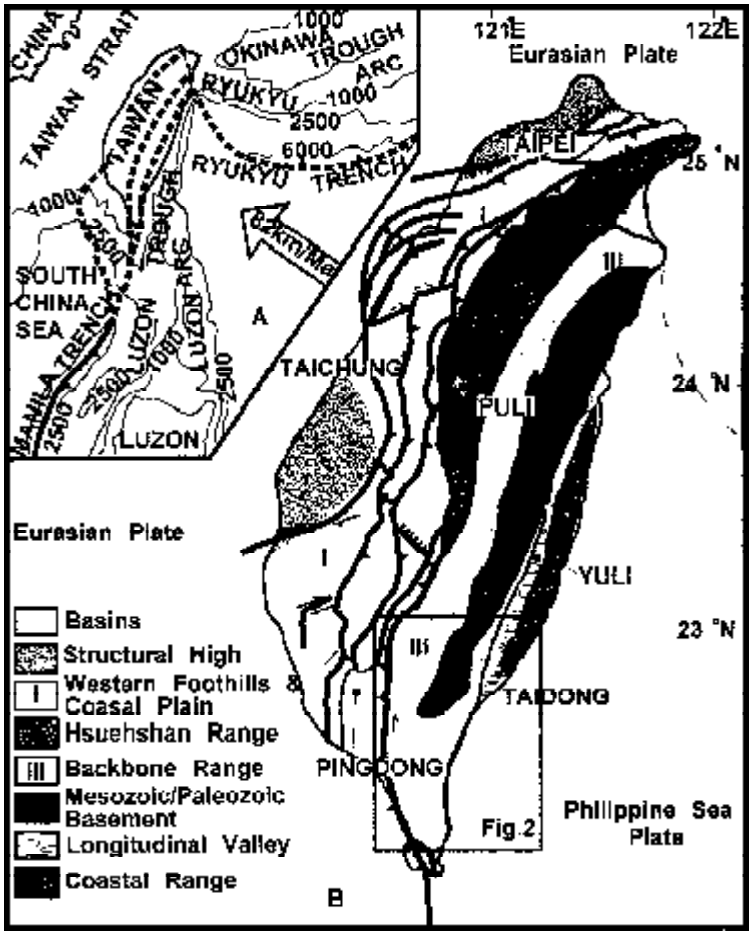

Figure 1. Geodynamic map of Taiwan mountain belt.

GEOLOGICAL SETTING

Southeastern Taiwan is underlain by thick series of Miocene accretionary wedge deposits, including dark gray argillites, and flysch deposits with occasional interbeds of gray compact sandstone and disseminated marly nodules (Hu *et al.*, 1981). They were metamorphosed under the prehnite-pumpellyite to lower greenschist facies during the Taiwan mountain building processes (Chen *et al.*, 1983) and exhibit intense layer parallel shearing with or without slaty cleavage (Pelletier and Hu, 1984). Considering the fact that the actual Luzon arc is still located to the east of the study area, these rocks could have already exposed and exhumed before the arc-continental collision during the such processes.

At a glance, the topographic map of southeastern Taiwan (Fig. 2A) may give one impression that a NE en-échelon pattern of rivers and ridges is well developed (Fig. 2B). This pattern seems to be the simplest structure than elsewhere in Taiwan. This particular topography is mainly controlled by regional structures of folding, thrusting left-lateral strike-slip faulting and erosion (Figs. 2B and C) resulted from transpressional tectonics (Fig. 2D).

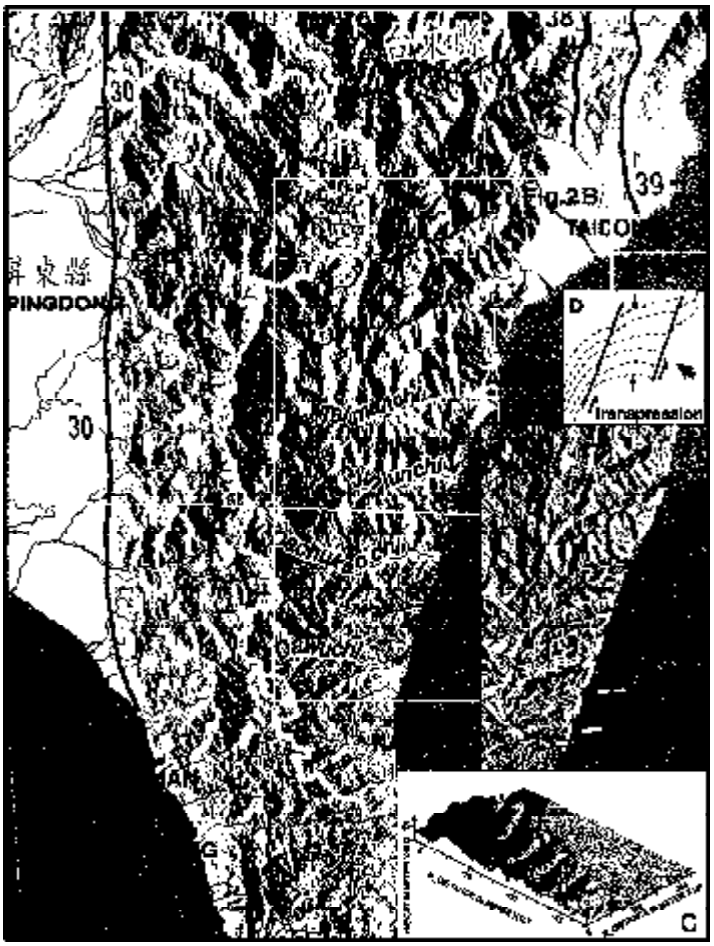

Figure 2. (A) Topographic map shows the study area and the well-aligned en-echelon structure pattern in the southeastern part of the Central Range. (B) Regional structures (C) Perspective view of (B). and (D) simplified interpretation of transpressional setting. Numbers: (1) Jinlun section, (2) Nantien section. Numbers in circle are active faults: (30) Chaochou Fault, (38) Luyeh Fault, (39) Southern Longitudinal Valley Fault.

In a section along the coast north of Jinlun (Fig. 2A section 1, Fig. 3), A refolded gently dipping fault zone of about 10m thick on the average is present all through the section. Here, sedimentary structures such as graded bedding, fluid cast, and cross bedding are common, allowing determination of polarity of bedding. In most cases, the strata underneath this fault zone are in normal sequence, whereas those above in this ~5 km profile were overturned. The cleavage is gently dipping in the argillites-dominated series, having the dip angle always smaller than that of bedding. In sandstone units, thicker >30cm, pressure solution type cleavage is generally sub-perpendicular to the bedding. Folding, antiform and synform, with wavelength ranging from 50 to 200m are widely distributed and can be traced along the valleys toward the west (Fig. 2C). Minor folds were strongly sheared into intrafoliated folds.

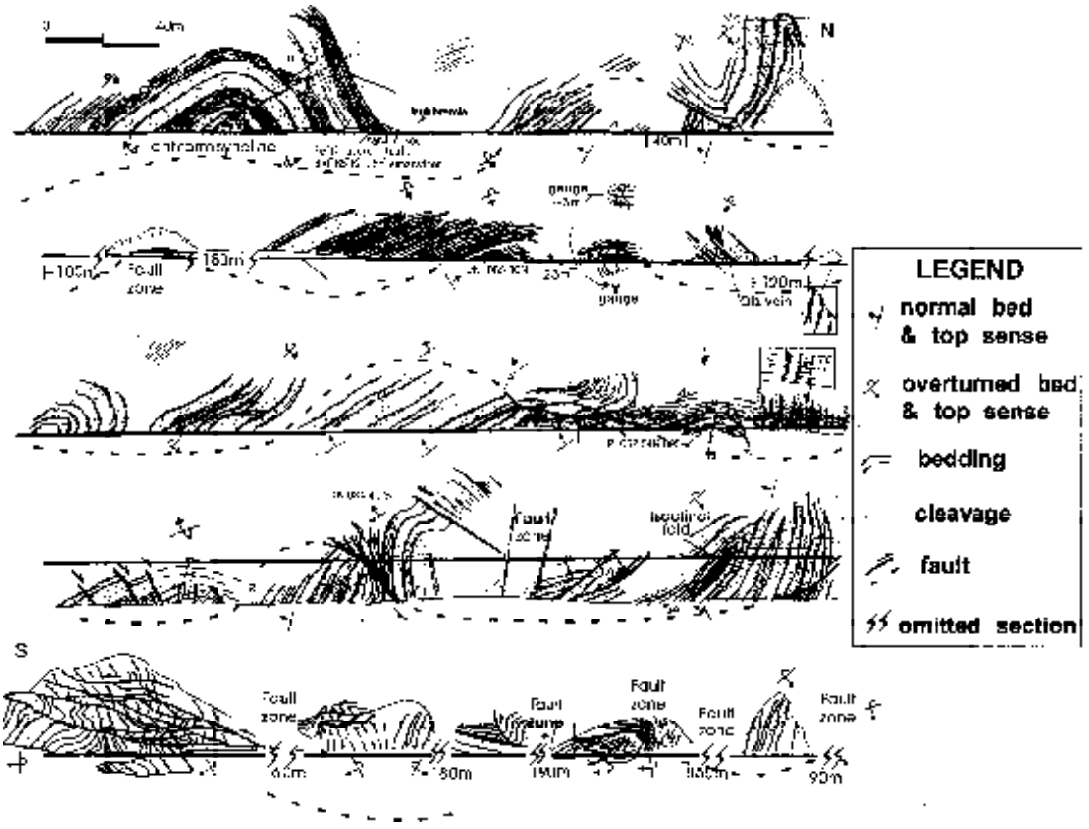

Figure 3. Five N-S (Continuous from right to left and top to bottom) structural sections of the Jinlun area (section 1 in Figure 2). JN: normal bedding. PI: possible reverse fault.

Along the E-W section south of Nantien (Figure 2A section 2, Figure 4), three generations of folding can be identified. The beddings were folded and refolded and mostly gentle dipping to the east. The earliest folding, F1, was indicated by a hook-type interference pattern. The foliation S1 associated with F1 might have been obliterated by later deformations. The fold axis of F1,

A1, trends 011/20N (Fig. 4 stereo-diagram). F2 fold is an isoclinal to tight folding overprinting F1 with foliation, S2, gently dipping to the east. In this area the S2 represents the most dominant cleavage and the fold axis of F2, A2, trends 063/45E. F3 fold is an upright folding with subvertical slaty cleavages in association with west-vergent intensive shear structures within the strata. The fold axis of F3, A3, trends 028/25N. Based on this overprinting relationship, the deformation stages can generally be grouped into three categories: west-vergent shearing and folding, east-vergent shearing and folding and left-lateral shearing and transpression. These deformation structures provide clues to reveal the deformation kinematics of the Central Range in the study area.

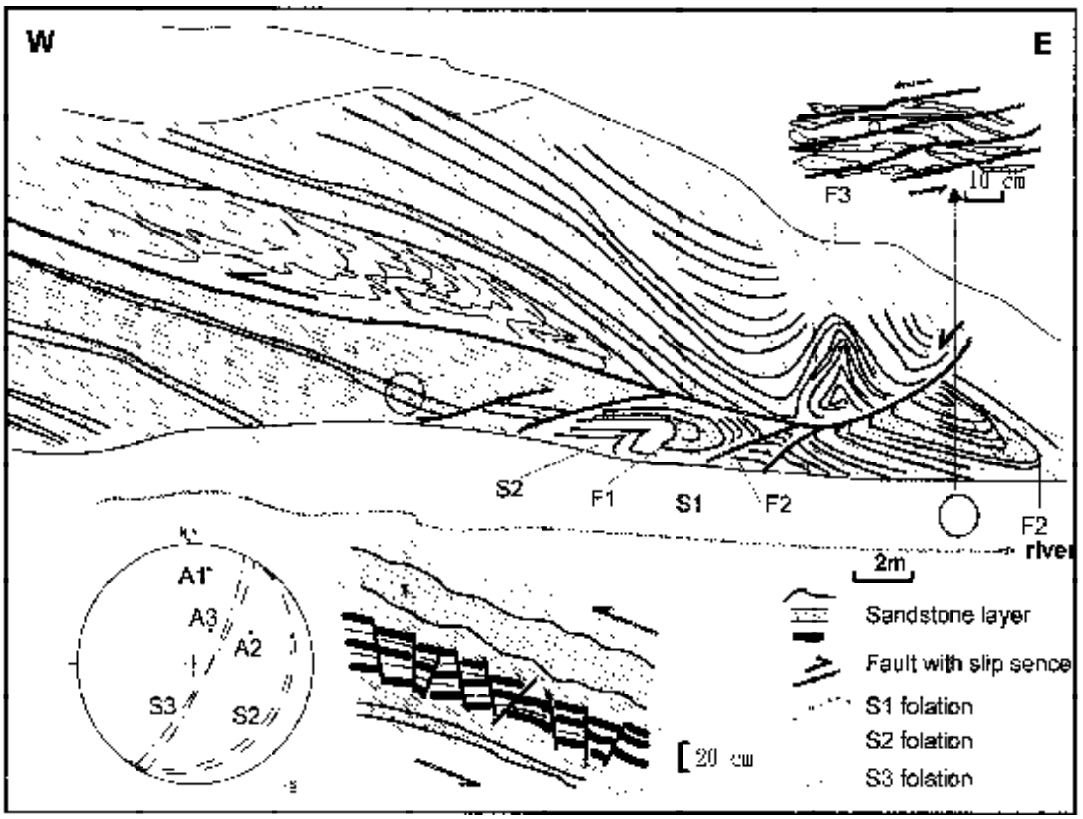

Figure 4. Structural section in the Lushan Formation of the Nantien area (Section 2 in Figure 2). Diagram shows lower hemisphere Schmidt projection of fold axial surfaces and axes, I.e. S2 and A2 for F2, S3 and A3 for F3, and A1 for F1. S1 is not shown because of strong deformation.

DEFORMATION STRUCTURES

West-vergent shearing and folding

As shown in Figure 5, west-dipping west-vergent shear structures mainly appear along the western boundary of the study area. West vergent asymmetrical tight to isoclinal folds are

in association with σ or δ type sheared quartz veins (Fig. 5B). The stretching lineation in company with this deformation stage (Fig. 6) is characterized by west-vergent (counterclockwise) thrust or drag fold (Figs. 6A and B,), and west vergent fragment rotation and quartz fibers (Figs. 6C and D).

Gentle east shearing and isoclinal folding

As one of the regional deformation products, East to southeast vergent shear structures are widespread along the eastern flank of the Central Range. The ductility of these structures generally decrease from north to south, reflecting the southward propagation of mountain building and southward migrating Quaternary exhumation of the metamorphic rocks due to oblique plate convergence. Therefore, the superficial east-vergent nappes structures were gradually obliterated by erosion toward the north. The best examples of these east-vergent ductile shear structures were well preserved in the Yuli areas (Figs. 1 and 7A). The outcrops showing brittle-ductile deformation are well exposed in the study area (Fig. 3, regional fault zone and Figs. 7B and D). Striations on the fault planes indicate the latest stage of shear movement being top to the SE or NE (Fig. 7C). The fault zones are generally associated with a large amount of breccias and gauges ranging in size from micro- to decimeters (Fig. 7D).

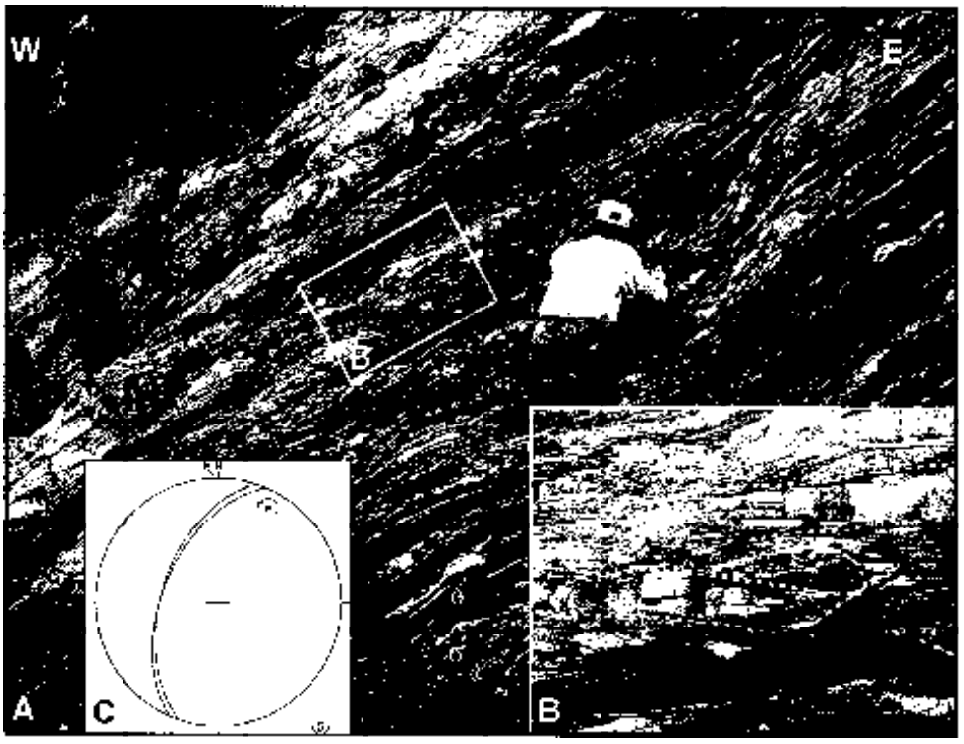

Figure 5. West-vergent and west-dipping shear structures in association with west vergent tight folds (Fig. 5B), Taimali river. (C). Lower hemisphere Schmidt projection of cleavage (S2, great circle) and axis (A2, solid dot) with rotational sense. σ and δ types shear structures are also indicated.

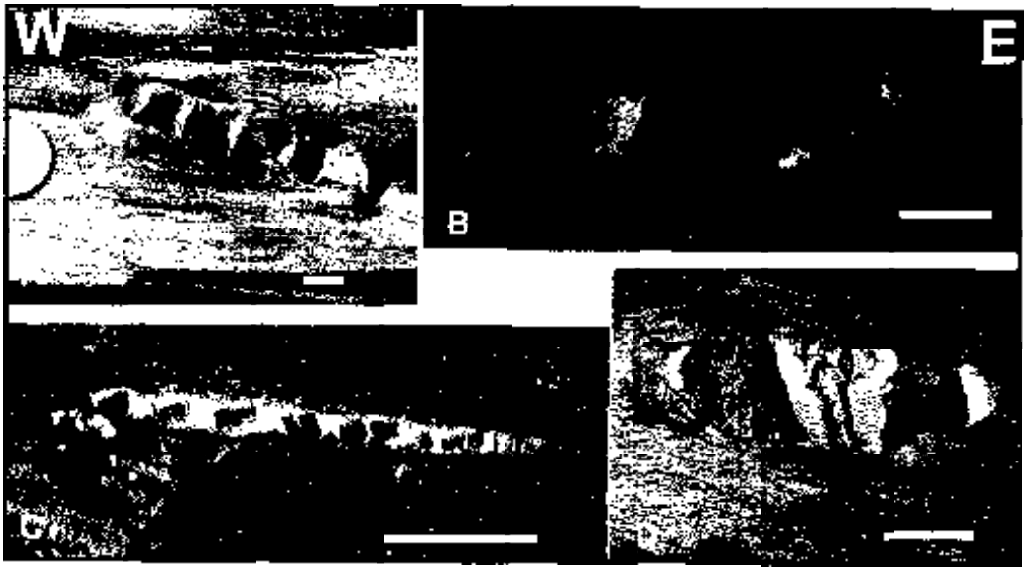

Figure 6. E-W oriented stretching lineation in association with the west-vergent structures. (A), (B) Stretched nodule in association with west-vergent thrust and drag fold respectively. (C), (D) Stretched fragments in association with west-vergent block rotation and curved fibrous vein . All white bars are 1 cm.

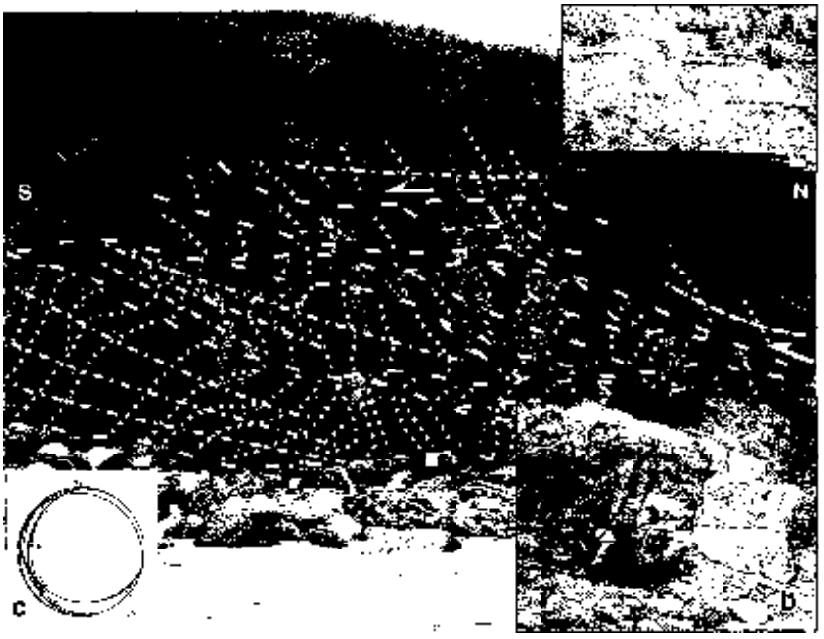

Figure 7. (A) E-vergent asymmetrical fold, north of Yuli (Figure 1, to the north of study area). (B) SE-vergent shear zones (dash lines) deformed beddings (dot lines) and S2 cleavages (dash-dot lines), north of Jinlun. (C) Lower hemisphere Schmidt projection of shear zones (great circle) and fault striations (arrows showing the movment direction of hanging wall) along the shear zone in (B) (D) Breccias and blocks in the shear zone.

Left-lateral shearing and transpression

N-S trending left-lateral shearing and transpression structures are most evident along the eastern border of the Central Range. They overprint the previous structures by left-lateral faulting (Fig. 8A) and also by densely distributed fracture cleavage (Fig. 8B). The transpression deformation described above (Fig. 2B) in association with left-lateral shearing result in mesoscale folding and thrusting. The wavelengths of folds ranges from 20 to 200m (Fig. 9). Cleavage pattern within these folds displays a very special fanning feature (Fig. 10). In sandstone layers, thicker than 15cm, the pressure solution cleavage is usually sub-perpendicular to the bedding. The bedding sub-parallel quartz veins in the inner arc part and the bedding perpendicular quartz veins in the outer arc part of thick sandstone bed demonstrate the fold in the sandstone was formed under conditions of pure tangential longitudinal strain (Ramsay and Huber, 1987). This indicated the fold is formed by flexure slip while the outer arc was under extension and the inner arc was under contraction deformation. However, in the shale dominated layers and sandstone/shale interbeds, the cleavages are dipping less than the bedding within the fold limbs (Fig.10). The sigmoidal pattern of cleavage within folded layers and quartz veins, thicker than about 0.5cm, between layers demonstrated that these folding experienced deformation of flexure-slip between layers and flexure-flow within layers. This cleavage pattern evidently suggests that it might be an earlier structure. Before transpressional folding, the early deformation developed penetrative cleavages sub-perpendicular to the bedding. This is followed by transpressional folding which deformed the cleavage to show this type of cleavage pattern (Fig. 10 B and C).

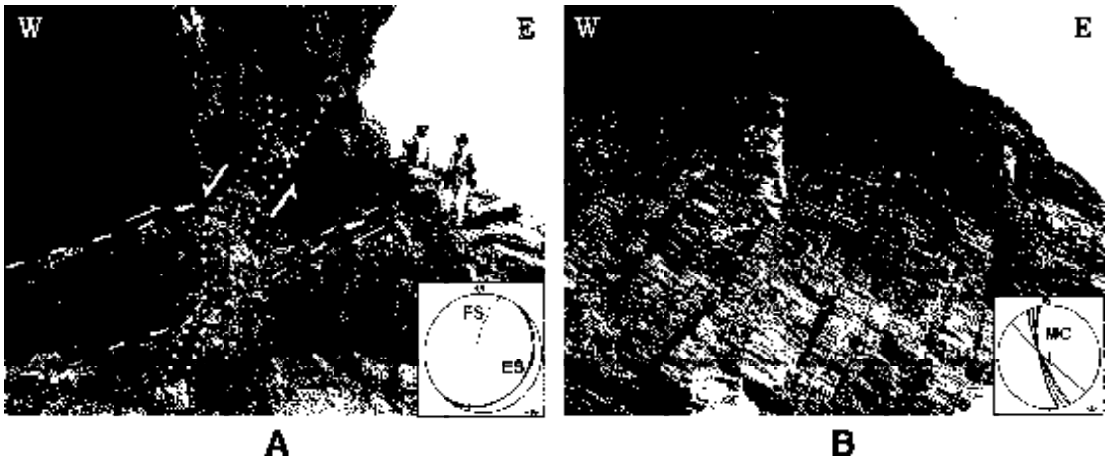

Figure 8. (A) East-vergent shear zone (framed by dash lines) is deformed by the N-S trending strike-slip fault zone (framed by dot lines). (B) N-S trending fracture cleavage in association with left-lateral and transpression tectonics. ES, FS and MC are great circles in lower hemisphere Schmidt projections of east-vergent shear zones and left-lateral strike-slip fault zone and fracture cleavage, respectively.

Figure 9. Antiform in the north of Jinlun.Sedimentary structures, graded bedding; flute cast, cross bedding and loading structures... etc indicate that the bedding was overturned before this folding.

Quartz veins

The quartz vein arrays in the study area show various kinds of beautiful local features (Fig.11), including pull-apart structures (Figs.11A and B), simple and deformed vein arrays (Figs.11 C and D), and conjugated en-echelon veins (Figs.11E and F). These may have formed at different deformation stages; as a consequence their patterns are very various and complicated. Structural analysis of some conjugated en-echelon vein arrays (Fig. 11E) show WNW-ESE compression direction. In Figure 11 F, the quartz veins were affected by the pressure solution cleavage and show the complicated pattern.

KINEMATICS

Microstructural analyses were carried out to characterize ductile structures and to reveal the kinematics of cleavage formation in the study area. Stretching lineations defined by phyllosilicates lie approximately parallel to the axes of regional folds with trends varying from northeast to east. Geometries of strain shadows indicate that (a) extension directions changed from along-strike (ENE-WSW) toward down-dip (NNW-SSE) and (b) top-to southwest or west-shearing generally occurred along strike direction. The regional-scale overturned sedimentary strata and the top-to southwest shearing suggest that rocks in the southeastern Central Range have experienced a left-lateral movement in the early stage and then have extruded upward and flipped upside down in the late stage. The whole deformation history can be summarized as fallows: (1) The first stage involves an early west-vergent contraction and volume loss stage that resulted in thrusting, regional tilting of strata slumping and west-vergent

folding (Figs.12A, B and C). (2) In the second stage the deformation is mainly dominated by general shear, resulting in widespread east-vergent back-folding and back-thrusting associated with isoclinal folding (Fig.12 D). (3) The third stage includes left-lateral shearing and transpression, in association with E-W contractional thrusting and folding, as well as penetrative spaced cleavage. This sequence of deformation is in accord with the exhumation mechanism of Backbone Range described by Yui and Chu (2000) and tectonics evolution suggested by Chemenda (1997) and Malavieille *et al.*, (1999) for the Taiwan Mountain building process.

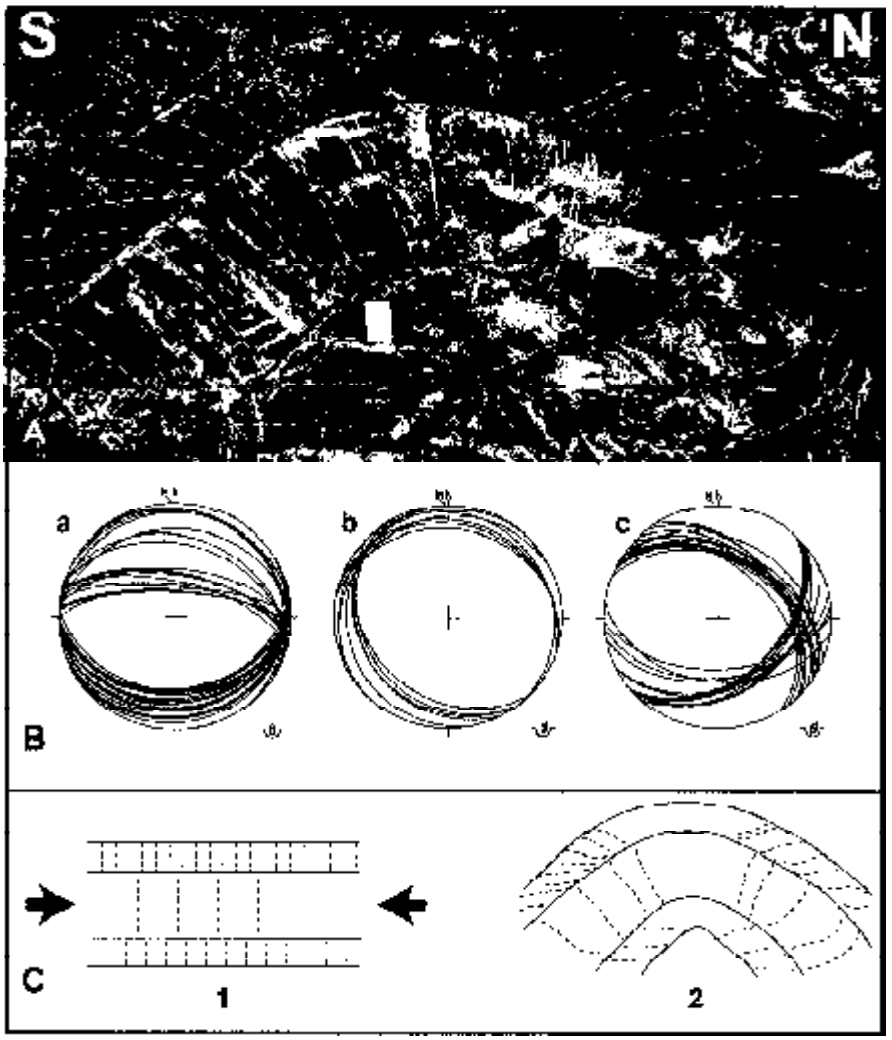

Figure 10. Cleavage style in the antiform of Jinlun area. (A). Closed up view and sketch of hinge part of Figure 9. B. Lower hemisphere Schmidt projections of bedding (a), slaty cleavage in shaly layers (b) and pressure solution cleavage in sandstone layers. (C) Interpretation of cleavage style formation from earlier (1) to present state (2).

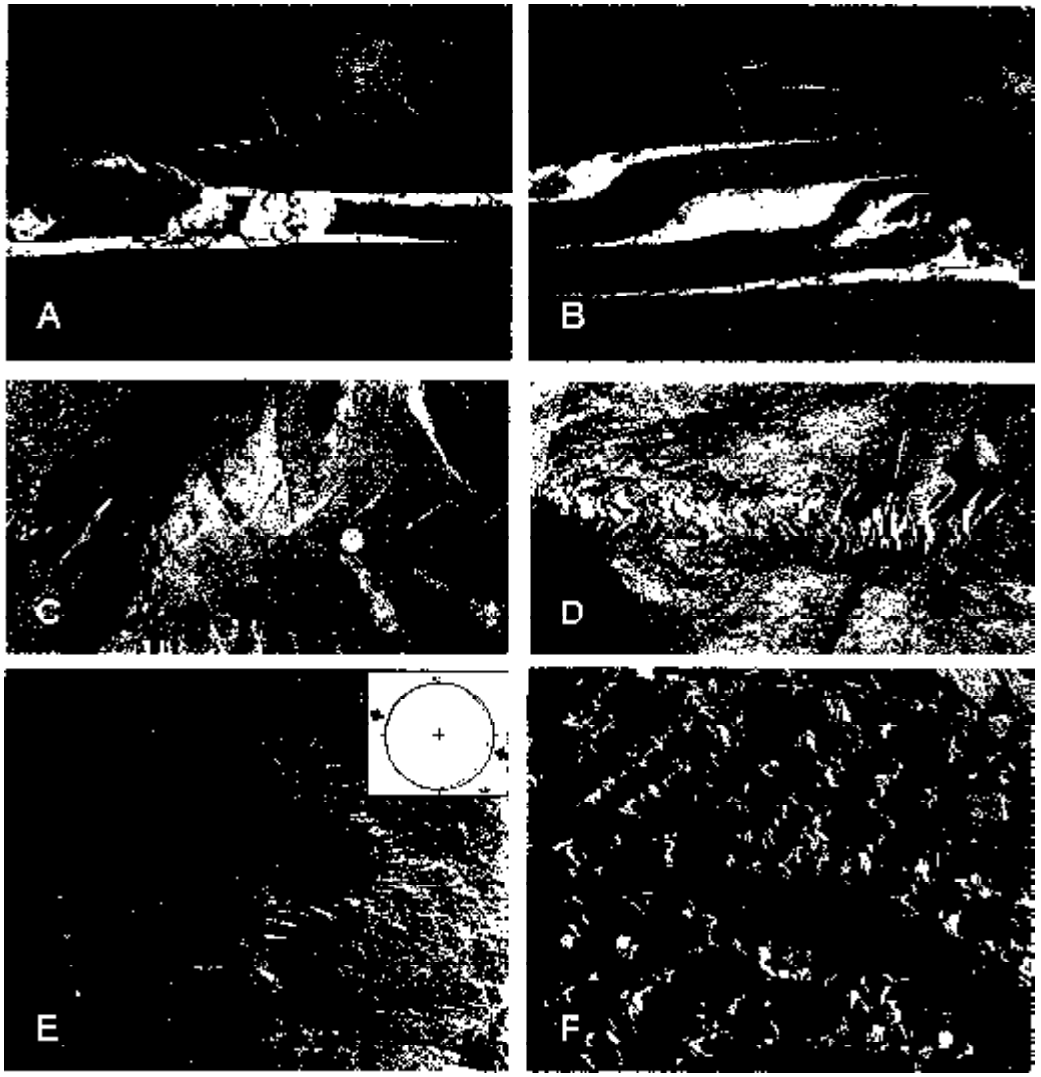

Figure 11. En-echelon quartz veins in the study area. (A), (B). En-echelon quartz veins in association with pull-apart structures. Simple (C) and deformed (D) left-lateral en-echelon veins. Conjugated en-echelon veins (E) and (F). In Figure F, the quartz veins were affected by the pressure solution cleavage and show the complicated pattern. Lower hemisphere Schmidt projections of vein array surface (great circle) in (E) indicate a WNW compression direction.

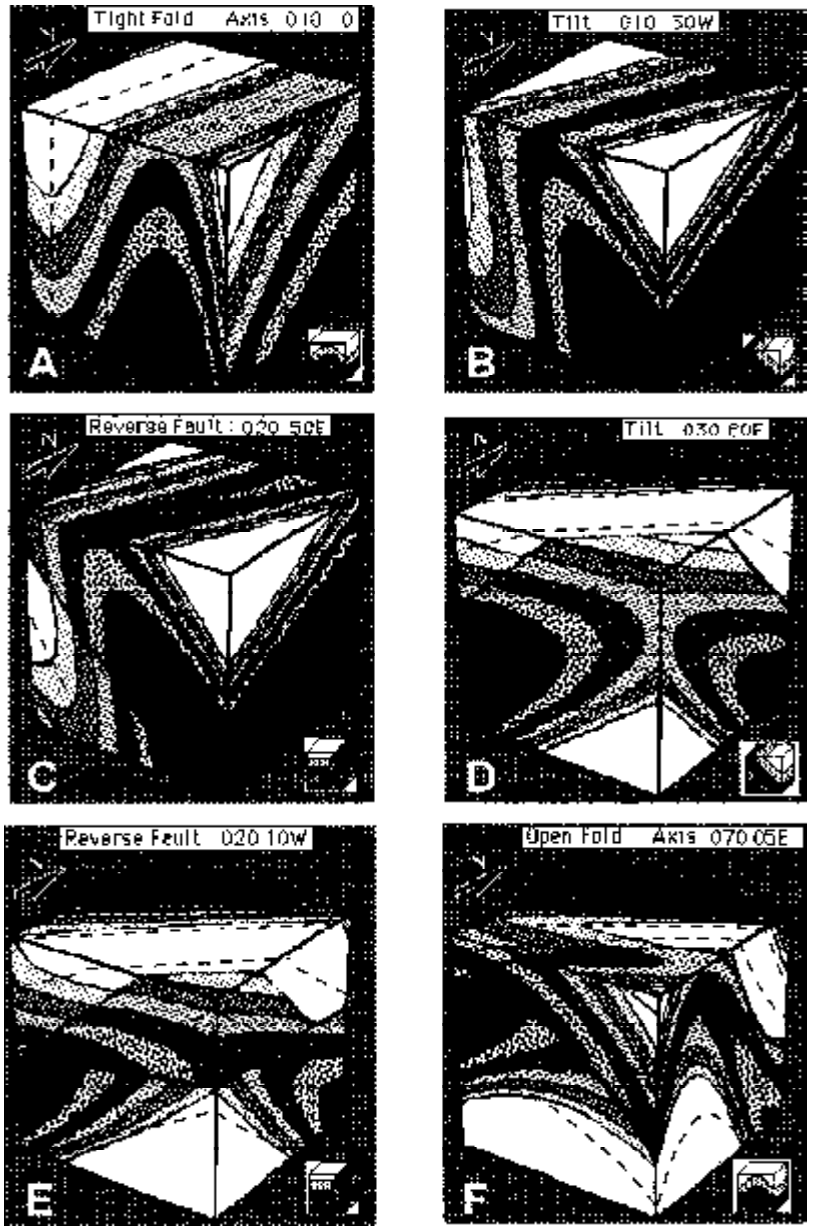

Figure 12. 3D diagrams illustrate the structural evolution of the study area: (A), (B), (C), demonstrate the early west-vergent contraction and volume loss stage that resulted in thrusting, regional tilting of strata slumping and W vergent folding, (D) shows the second stage dominated by general shear, that resulted in widespread east-vergent back-folding and back-thrusting associated with isoclinal folding (E), (F) shows the third stage of transpression, in association with E-W contractional thrusting and folding, as well as the formation of penetrative spaced cleavage. (Diagrams produced by Macintosh software Geostructure 1.0, Aspinwall and Wu, 1986).

CONCLUSIONS

1) Transpressional structures are penetratively distributed in southeastern Taiwan.

2) Rapid uplift and exhumation of the metamorphic rocks in southeastern Taiwan demonstrate that the arc-continental collision is not sufficient for explaining the Taiwan Mountain building processes.

3) Active progressive oblique convergence, accretion of the north Luzon arc and erosion may have been responsible for the elongation of longitudinal valley and the complex deformation structures to the north of Taidong.

ACKNOWLEDGMENTS

This study was supported by the National Science Council grant (NSC89-2116-M002-016). The first author thanks Lo, Ching-Hua, Yeh, En-Chao and two reviewers Chu, Hao-Tsu and Lee, Chy-Ti for revising the manuscript.

REFERENCES

Aspinwall, D. and Wu, S.F. (1986) Geostructure 1.0. Courseware Development Group, Dartmouth Collage.

Biq, Ching chang (1971) A fossil subduction-zone in Taiwan: *Proc. Geol. Soc. China*, **14**, 146-154.

Biq, Chingchang (1972) Duel-trench structure in the Taiwan-Luzon region: *Proc. Geol. Soc. China*, **15**, 65-75.

Chai, B. H. T. (1972) Structural and tectonic evolution of Taiwan: *Am. J. Sci.*, **272**, 389-422.

Chemenda, A.I. (1997) Evolutionary model for the Taiwan collision based on physical modelling: *Tectonophysics*, **274**, 253-274.

Chen, C. H., Chu, H. T., Liou, J. G., and Ernst, W. G. (1983) Explanatory notes for the metamorphic facies Map of Taiwan: *Spec. Publ. Cent. Geol. Surv.*, **2**, 1-3.

Hu, H. N., Chu, H. T., and Jeng, R. C. (1981) The "slate formation" of Southern Taiwan: Preliminary Result: *Bull. Cen. Geol. Surv.*, **1**, 33-49.

Malavieille, J., Lallemand, S. E., Dominguez, S., Deschamps, A., Lu, C. Y., Liu, C.-S., Schnurle, P., Angelier, J., Collot, J. Y., Deffontaines, B., Founier, M., Hsu, S. K., Le Formal, J. P., Liu, S. Y., Sibuet, J. C., Thareau, N., and Wang, F. (2000) Geology of arc-continent collision in Taiwan: Marine observation and geodynamic model: *GSA special paper*, in press.

Pelletier, B., and Hu, H. N. (1984) New structural data along two transects across the southern half of the Central Range of Taiwan: *Mem. Geol. Soc. China*, **6**, 1-19.

Ramsay, J.G. and Huber, M.I. (1987) Folds and faults. The Techniques of Modern Structural Geology: *Academic Press*, **2**, 695 pp.

Suppe, J. (1981) Mechanics of mountain building in Taiwan: *Mem. Geol. Soc. China*, **4**, 67-89.

Yu, S. B., Chen, H. Y., and Kuo, L. C. (1997) Velocity field of GPS stations in the Taiwan area: *Tectonophysics*, **274**, 41-49.

Yui, T.-F., and Chu, H.-T. (2000) 'Overturned' marble layers: evidence for upward extrusion of the Backbone Range of Taiwan: *EPSL*, **179**, 351-361.